Histamine H4 receptor antagonism prevents the progression of diabetic nephropathy in male DBA2/J mice.

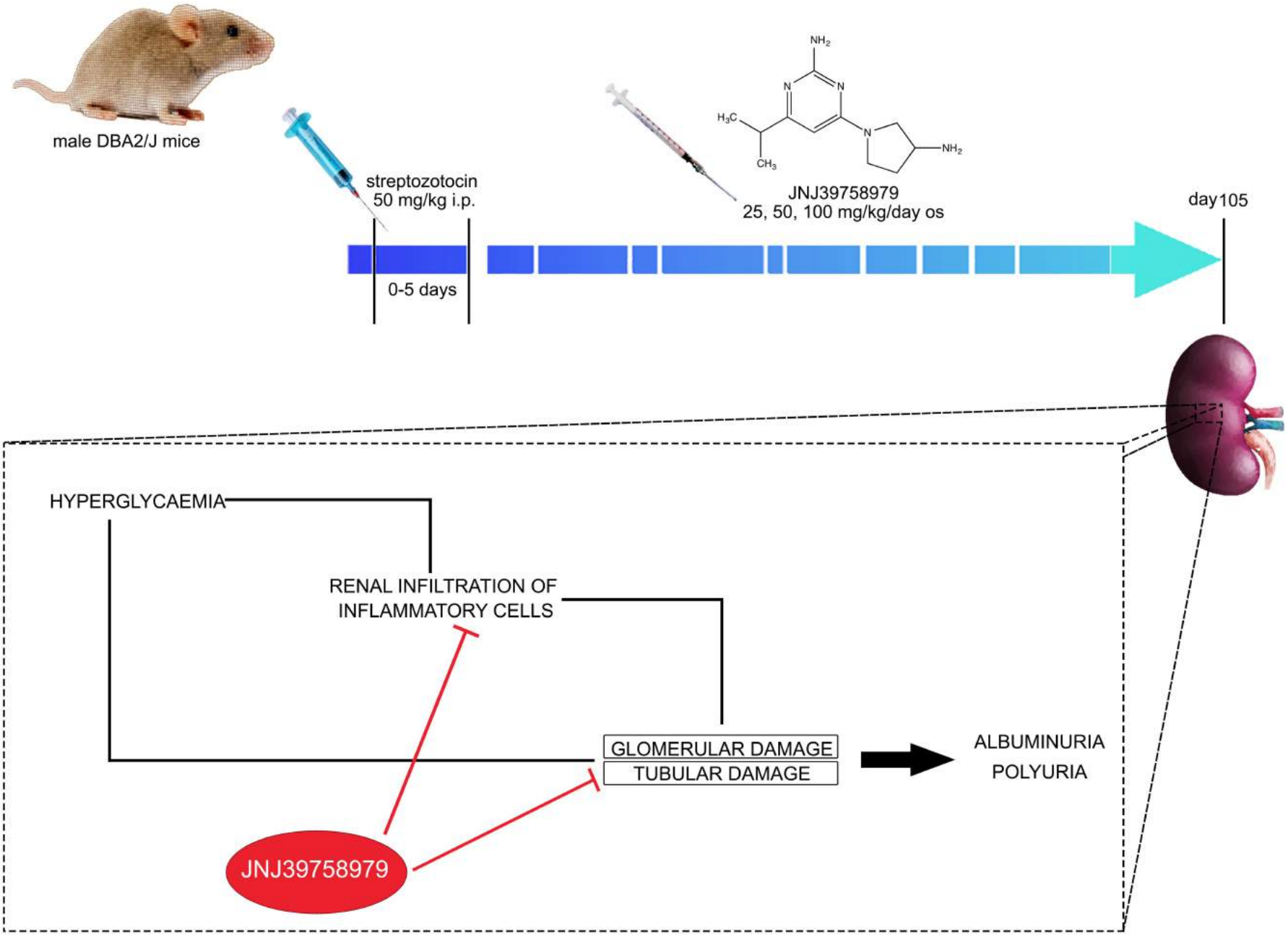
male DBA2/J mice
streptozotocin
50 mg/kg i.p.
JNJ39758979
25, 50, 100 mg/kg/day os
day 105
0-5 days
HYPERGLYCAEMIA
RENAL INFILTRATION OF
INFLAMMATORY CELLS
GLOMERULAR DAMAGE
TUBULAR DAMAGE
ALBUMINURIA
POLYURIA
JNJ39758979

Abstract

Due to the incidence of diabetes and the related morbidity of diabetic nephropathy, identification of new therapeutic strategies represents a priority. In the last few decades new and growing evidence on the possible role of histamine in diabetes has been provided. In particular, the histamine receptor H_4R is emerging as a new promising pharmacological target for diabetic nephropathy. The aim of this study was to evaluate the efficacy of selective H_4R antagonism by JNJ39758979 on the prevention of diabetic nephropathy progression in a murine model of diabetes induced by streptozotocin injection. JNJ39758979 (25, 50, 100 mg/kg/day p.o.) was administered for 15 weeks starting from the onset of diabetes. Functional parameters were monitored throughout the experimental period.

JNJ39758979 did not significantly affect glycaemic status or body weight. The urine analysis indicated a dose-dependent inhibitory effect of JNJ39758979 on Albumin-Creatinine-*Ratio*, the Creatinine Clearance, the 24 h urine volume, and pH urine acidification ($P < 0.05$). The beneficial effects of JNJ39758979 on renal function paralleled comparable effects on renal morphological integrity. These effects were sustained by a significant immune infiltration and fibrosis reduction. Notably, megalin and sodium-hydrogen-exchanger 3 expression levels were preserved.

Our data suggest that the H_4R participates in diabetic nephropathy progression through both a direct effect on tubular reabsorption and an indirect action on renal tissue architecture via inflammatory cell recruitment. Therefore, H_4R antagonism emerges as a possible new multi-mechanism therapeutic approach to counteract development of diabetic nephropathy development.

Keywords: kidney; diabetes; histamine, histamine H_4R antagonist, JNJ39758979, diabetic nephropathy

Non-standard Abbreviations

ACR = Albumin-Creatinine-*Ratio*; AQP= Aquaporin; CrCl = Creatinine Clearance; ESRD = End Stage Renal Disease; GBM = Glomerular Basement Membrane; HDC = Histidine Decarboxylase; H&E = Haematoxylin and Eosin; HPLC = High Performance Liquid Chromatography; H_{1-4}Rs = Histamine H_{1-4} Receptors; IL = Interleukin; IP = Interferon gamma-induced Protein; LRP-2 = low

density lipoprotein-related protein-2 (megalin) gene; MCP = monocyte chemoattractant protein; NHE3 = Sodium-Hydrogen Exchanger 3; OKP cells = Opossum Kidney Cells; PAS = Periodic Acid Schiff; PMNs = Polymorphonuclear Neutrophils; RAS = renin-angiotensin-system; RT = reverse-transcription; SD = Slit Diaphragm; STZ = streptozotocin; TGF-ß = Transforming Growth Factor-ß; THP = Tamm–Horsfall glycoprotein; UPE = Urinary Protein Excretion

1 Introduction

The incidence of diabetes is expected to exceed 592 million by 2030 [1], is alarmingly increasing the rate of microvascular complications including diabetic nephropathy.

With about one-third of diabetic patients developing diabetic nephropathy, this complication is one of the most important challenges to clinical and public health [2]. Despite the benefits afforded by a therapy mainly based on the modulation of the renin-angiotensin system (RAS) [3], incidence of the overall progression of diabetic nephropathy remains unacceptably high [4]. Haemodialysis and transplantation are the only therapeutic options available when End Stage Renal Disease (ESRD) occurs. Therefore, to improve health outcomes and reduce the societal burden, the pursuit of innovative effective therapeutic strategies for the treatment of diabetic nephropathy is clearly warranted.

Interestingly, histamine is emerging as a new mediator in diabetic nephropathy [5]. Histamine is a pleiotropic amine, historically implicated in several immune-inflammatory processes. It acts through four subtypes of G-protein coupled receptors, named histamine H_{1-4} receptors (H_{1-4}Rs), which are differentially expressed in various organs, including the kidney included [6-9]. Histamine synthesis is catalysed by the rate-limiting enzyme histidine decarboxylase (HDC), mainly expressed in the "professional" mast cell. However, HDC has been also found in the proximal tubule and human podocytes [9-11]. Actually, the first evidence for a possible role of histamine in diabetic nephropathy was provided in the 1960s when, concurrent with an increased tissue HDC activity, an increased level of this amine was observed in the kidney of diabetic animals [12, 13]. In particular, histamine has already been demonstrated to increase salt and water excretion [14-16] and renin release [17], and to decrease the ultrafiltration coefficient [18]. These effects were classically attributed to the well-known vasoactive properties of the amine. However, different lines of evidence point out to a potential direct contribution of histamine to the renal pathophysiology, far beyond its effect on glomerular microcirculation hemodynamic [5]. Histamine was found to increase fasting-induced apoptosis in tubules [19]. Moreover, the increased number of the tubulointerstitial mast cells and their degranulation consequent to diabetic nephropathy progression are suggestive of a direct contribution by histamine to renal inflammation and fibrosis [19, 20]. The use of a mast cells stabiliser afforded protection against renal dysfunction in a high fat diet rat model [21].

Recently, compelling evidence pointing to the H_4R as a possible target for diabetic nephropathy was provided. We reported both the H_4R expression on epithelial tubular cells [8] and its significant over-expression in the kidney of diabetic rats [6]. Moreover, our pilot data are indicative of a positive correlation between renal H_4R expression and albuminuria in a model of murine diabetes [22]. Therefore, the intriguing potential of H_4R antagonism as a new pharmacological and therapeutic approach for diabetic nephropathy has become evident.

In comparison to other the different selective H_4R antagonists, JNJ39758979 [(*R*)-4-(3-amino-pyrrolidin-1-yl)-6-isopropyl-pyrimidin-2-ylamine][23] offers the following advantages: (*i*) is orally bioavailable; (*ii*) has a long half life (126-157 h for a single dose); (*iii*) rapidly reaches the kidney

(mean t_{max} 2.0 h), from which it is slowly eliminated (22.3 h; kidney to plasma *ratio* 95.8); (*iv*) is metabolically stable ($t_{1/2}$ *in vitro* 120 min); (*v*) does not inhibit the cytochrome P450 (CYP) isoforms; (*vi*) have a low fluctuation index (from 0.852 to 2.60) thus allowing a once daily chronic administration [24]. Therefore, the primary aim of this study was to evaluate whether JNJ39758979 is able to preserve renal morphological and functional integrity in a murine model of diabetic nephropathy.

2 Methods

2.1 Materials

All chemicals, not otherwise indicated and rabbit polyclonal anti-β-actin antibody (A2066), were from Sigma Aldrich (St. Louis, MO, USA). JNJ39758979 was synthesised by Janssen Research & Development, LLC as previously described [23].

The Glucocard MX Blood Glucose Meter was from A. Menarini Diagnostic (Florence, IT). The Albumin enzymatic immunoassay kits ELISA Quantitation Set was from Bethyl Laboratories, Inc. (Montgomery, TX, USA).

The goat polyclonal anti-Megalin (sc-515750, lot number L2104), the goat polyclonal anti-H$_1$R (sc-33967, lot number L0913) the rabbit polyclonal anti-aquaporin (AQP)1 (sc-20810, lot number B0210), the rabbit polyclonal anti-Tamm–Horsfall glycoprotein (THP; sc-20631, lot number A0611) and the rabbit polyclonal anti-AQP2 (sc-28629, lot number G1713) antibodies were from Santa Cruz Biotechnology (Dallas, Texas, USA), the rabbit polyclonal anti-NHE3 (GTX41967, lot number 821700650) was from Gentex (San Antonio, TX, USA). The rabbit peroxidase-labelled secondary antibody was from Cell Signaling Thecnology, Inc. (Danvers, MA, USA). The donkey anti-goat Fluor 568- conjugated IgG was purchased from Thermofisher Scientific (Waltham, MA, USA), while the Alexa Fluor 594 AffiniPure bovine anti-goat and the Alexa Fluor 488 AffiniPure donkey anti-rabbit were from Jackson ImmunoResearch Laboratories, Inc. (West Grove, PA, USA). TRIzol Reagent, the Taqman gene expression assay reagents and probes, the Optical 96-well plates and the micro-BCA™ Protein Assay Kit were from Thermofisher Scientific. The cDNA Synthesis Kit and the ECL substrate were from BioRad (Foster City, CA, USA). The nitrocellulose membranes were from GE Healthcare life Sciences (Milano, IT).

2.2 Animal Care and ethics statement

Five-six week old (20.74 ± 2.58 g body weight) male DBA2/J mice (Charles River Laboratories, Calco, IT) were maintained in compliance with the European Directive 2010/63/EU on the protection of animals used for scientific purposes, housed in a controlled environment at 25 ± 2°C with alternating 12-hour light and dark cycles and fed with a standard diet during a 1-week adaptation period, fed with a standard pellet diet (Piccioni, Settimo Milanese, Milan, IT) and watered *ad libitum*. The scientific project was approved by the "Animal Use and Care Committee'' of the Turin University. In order to reduce the number of animals, the minimum sample size of 10 animals/group, randomly assessed according to a simple randomisation design, was determined by

applying the Fleiss test for an unmatched case-control study as power analysis [25]. Confidence interval was 90%, and the power was at 85% and the alpha level was set at 0.05. This design provides the power to investigate the differences in renal function between, not only normal and diabetic control mice, but also between diabetic and treated mice.

2.3 Induction of diabetes

Hyperglycaemia was induced in DBA2/J 7-8 week old mice (this inbred mouse strain being the most susceptible to diabetic nephropathy) by multiple low-dose streptozotocin (STZ)-injection (50 mg/kg day STZ freshly made in 0.1 mol/l citrate buffer, pH 4.5) i.p. for 5 consecutive days, thus to avoid acute STZ toxicity, according to the Animals Models of Diabetic Complications Consortium guidelines (available at http://www.amdcc.org). Control animals were treated with vehicle alone. The onset of diabetes was evaluated by measuring 6 h fasting blood glucose. Blood glucose was then measured fortnightly using a Glucocard MX Blood Glucose Meter. Weight, food and water intake were recorded on a weekly basis. Diabetes was defined as fasting blood glucose level ≥ 200 mg/dl. After the onset of diabetes, the selective H_4R antagonist JNJ39758979 was administered daily for 15 weeks as a water solution by oral gavage at 25, 50, 100 mg/kg. Fifteen weeks after diabetes onset, mice were anaesthetised with isofluorane and killed by cardiac exsanguination; blood and kidneys were collected for biochemical and morphological analyses. Data recording and data analysis were blinded to both the operators and the analysts, with only the individual administered the drug aware of the drug treatments given. Moreover, animal specimens were randomly labelled by a unique numeric code by AP and ACR, to guarantee blind tissue sample processes.

2.4 Renal function evaluations

Twenty-four-hours urine collection was performed using metabolic cages. Urine volume and pH were determined. All analyses were run in triplicate. Proteinuria was measured by the Bradford method using Bovine Serum Albumin as standard [26]. Albuminuria was determined by ELISA, according to the manufacturer's instruction; the analysis was performed in duplicate.

Creatinine was determined by a High Performance Liquid Chromatography (HPLC) reverse phase method [27, 28]. A more comprehensive description is found in Supplementary materials.

2.5 Morphological analysis

Renal samples collected at sacrifice were fixed by immersion in 4% paraformaldehyde, dehydrated in graded ethanol, paraffin embedded and cut in 5 µm thick sections. Histological slides were stained with haematoxylin and eosin (H&E) to evaluate alterations of gross tissue architecture; with periodic acid Schiff (PAS) to quantify glomerular damage; and 0.1% picrosirius red for the renal collagen content assessment. Stained sections were examined and pictures were taken with a Zeiss Axioskop microscope (Zeiss, Mannheim, DE) at 25X, 100X or 10X magnification, respectively. Morphological measurement details have been provided in Supplementary Materials.

2.6 Immunofluorescence analysis

Megalin immunoreactivity was determined on 5 µm thick tissue sections. The sections were deparaffinised and re-hydrated, followed by microwave antigen retrieval in 10 mM sodium citrate, pH 6.0. After incubation in 1.5% bovine serum albumin in PBS, pH 7.4 for 20 min at RT to minimise non-specific binding, renal sections were incubated overnight with goat polyclonal anti-Megalin (1:50). The immunoreactions were revealed by incubation with donkey anti-goat Fluor 568-conjugated IgG (1:350) for 2 h at RT. Negative controls were carried out by omitting the primary antiserum. The immunoreaction products were observed under an epifluorescence Zeiss Axioskop microscope at 40X magnification and quantified as described in Supplementary Materials. For the co-localization analysis, after antigen retrieval (sodium citrate 10 mM pH 6.9 for 3 cycles of 20 s in microwave 750 W) and blocking, the sections were incubated overnight with goat polyclonal anti-H_4 receptor and rabbit polyclonal anti-THP, anti-AQP1 or anti-AQP2 (1:50) antibodies, followed by incubation with the Alexa Fluor 594 AffiniPure bovine anti-goat or the Alexa Fluor 488 AffiniPure donkey anti-rabbit. After counterstaining with DAPI, photomicrographs were obtained by Apotome systems (Zeiss) using a x40 objective.

2.7 Transmission Electron Microscopy

The preparation of the renal biopsies for electron microscopy was performed according to standardised procedures. The sample were cut into 1 mm^3 pieces, fixed in 4% glutaraldehyde (phosphate buffered, pH 7.2) and 1% osmium tetroxide and embedded in Epon 812 (Fluka-Sigma-Aldrich, Milan, IT). After ultra-thin sectioning, the samples were post-stained with uranyl acetate and alkaline bismuth subnitrate and examined under a JEM 1010 electron microscope (Jeol, Tokyo, JP) at 80 kV. At least two glomeruli were analysed from each sample. To quantify the ultrastructural alterations of the filtration barrier, the number of slit diaphragms and foot processes per 10 µm and the foot processes base width, were measured. The counting was performed on a randomly determined area of the glomerular capillary wall. To test the reliability of the morphological analysis, the measurements were carried out twice.

2.8 qPCR

One hundred micrograms of total RNA, extracted according to Supplementary Materials, was reverse transcribed to single-stranded cDNA using the commercially available i-script cDNA Synthesis Kit, according to the manufacturer's instructions. Negative controls of the reverse-transcription (RT) were carried out omitting the enzyme or substituting RNA with RNAse-free water, to exclude DNA or RNA contamination, respectively. qPCR for the quantification of the transcript level of low density lipoprotein-related protein (LRP)-2 was performed using the ABI Prism 7500 Sequence Detection System instrument (Thermofisher Scientific) and hydrolysis probes (Mm01328171_m1). PCR amplifications, run in triplicate, were performed in Optical 96-well plates on cDNA samples corresponding to a final RNA concentration of 50 ng. In each run blank controls, no template (water) or RT-negative reactions, were performed. Quantification cycle Cq values were analysed. All values were normalised to the 18S ribosomal reference gene (Mm02601777_g1)

using the $2^{-\Delta\Delta Cq}$ method and fold-change expression with respect to control was calculated for all samples.

2.9 Immunoblotting

Kidney specimens randomly selected from 5 animals/group were lysed in cold buffer (10 mM Tris/HCl pH 7.4, 10 mM NaCl, 1.5 mM, MgCl2, 2 mM Na2 EDTA, 1% Triton X-100), supplemented with 10× Sigmafast Protease Inhibitor cocktail tablets. Total protein content was measured spectrophotometrically using a micro-BCA™ Protein Assay Kit. Sixty microgram of total proteins were randomly electrophoresed by SDS-PAGE and blotted onto nitrocellulose membranes. The membranes were incubated overnight at 4°C with rabbit polyclonal anti-sodium-hydrogen exchanger (NHE)3 (1:1000) and rabbit polyclonal anti-β-actin antibodies (1:20000), assuming β-actin as control invariant protein. Specific bands were detected using rabbit peroxidase-labelled secondary antibody (1:2000) and enhanced chemiluminescent (ECL) substrate. Densitometric analysis was performed by ImageJ 1.41 (NIH, USA) software. Fold-change expression with respect to control was calculated for all samples.

2.10 Statistical analysis

For each assay, data were reported as mean values (± standard error of the mean, S.E.M.) of individual average measures of the different animals per group. The test for normality using the Kolmogorov-Smirnov followed by the one-way ANOVA and the *post hoc* Tukey test for multiple comparisons were performed when there was a variance homogeneity, otherwise for the LRP-2 and HNE3 relative expression the non-parametric Kruskal-Wallis test was used. Calculations were made with Prism 5 statistical software (GraphPad Software, Inc., San Diego, CA, USA). A probability value (P) of < 0.05 was considered significant.

3 Results

3.1 Effect of JNJ39758979 on blood glucose level and body weight

One week after the last STZ injection, more than half of DBA2/J mice developed a hyperglycaemic status (≥ 200 mg/dl), compatible with the definition of diabetes in mice [29]. The glycaemic level increased to over 200 mg/dl in all the diabetic animals ($n = 40$) within 21 days, remaining severe ($P < 0.05$ *vs* control) throughout the experimental period. No statistical difference in hyperglycaemia was observed between the diabetic groups, with JNJ39758979 not affecting the glycaemic status, irrespective of the dose treatment (Fig. 1a).

Consistently with the glycaemic status, only the control animals displayed an increase in body weight, whereas the STZ mice body weights were significant reduced irrespectively of the drug treatment ($n = 10$/group, $P < 0.05$ *vs* control; Fig. 1b). No insulin treatment was administered during the study in any mouse.

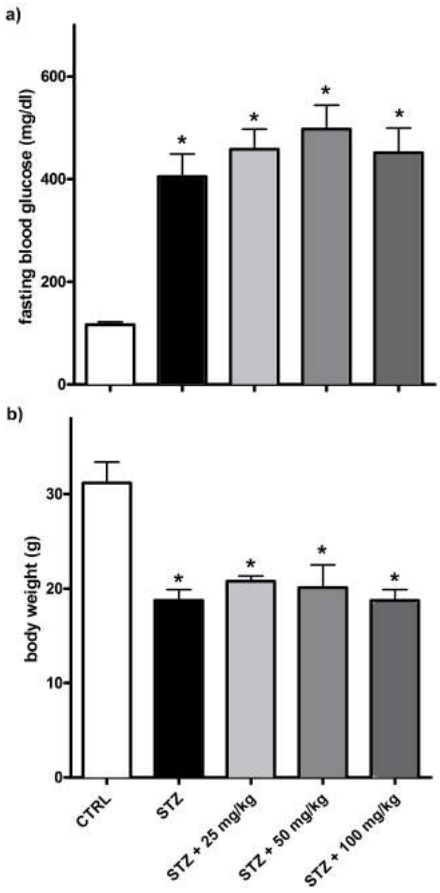

Fig. 1. Effect evoked by JNJ39758979 on metabolic parameters at 15 weeks after diabetes onset. Six hour fasting glucose level (**a**) and body weight (**b**) measurements. Data are expressed as the mean ± S.E.M. (n = 10/group); *P < 0.05 *vs* CTRL.

3.2 JNJ39758979 preserves renal function

The urine analysis at 15 weeks of diabetes showed a dose-response beneficial effect of JNJ39758979. The urine volume, robustly increased in STZ mice, was dose-dependently reduced in JNJ39758979-treated mice. JNJ39758979 at 100 mg/kg also restored the water to urine *ratio* to control levels (Table 1). Moreover, mice treated with JNJ39758979 at 100 mg/kg showed a significant increase in urine pH compared to STZ mice (Table 1). Most notably, diabetic animals showed a significant increase in Urinary Protein Excretion (UPE), Albumin-Creatinine-*Ratio* (ACR) and a parallel significant drop in the Creatinine Clearance (CrCl), suggestive of a renal failure coherent with the duration of severe hyperglycaemia. JNJ39758979 at the highest dose was effective in ameliorating UPE and restoring the ACR and the CrCl to the control level (Table 1)

Table 1. Renal Function parameters at week 15 after diabetes onset

Treatment	Urine volume/24 h (mL)	Urine pH	Water to Urine *ratio* (%)	UPE (mg/24 h)	ACR (μg/mg)	CrCl (ml/min)
CTRL	0.51 ± 0.22	6.27 ± 0.12	25 ± 4.03	3.29 ± 0.38	27.73 ± 9.00	0.11 ± 0.01
STZ	28.00 ± 3.15*	5.16 ± 0.10*	78.4 ± 9.78*	96.78 ± 8.79*	524.68 ± 60.52*	0.02 ± 0.00*
STZ + JNJ 25 mg/kg	20.57 ± 8.71*	5.10 ± 0.10*	55.74 ± 12.19*	74.69 ± 3.67*	439.06 ± 116.14*	0.04 ± 0.01*
STZ + JNJ 50 mg/kg	18.00 ± 4.24#	5.20 ± 0.11*	52.50 ± 8.78*	55.93 ± 2.53*#	255.58 ± 33.93*#	0.06 ± 0.02*
STZ + JNJ 100 mg/kg	10.00 ± 0.53#	5.76 ± 0.12*#	32.56 ± 5.12#	41.62 ± 5.69*#	36.04 ± 10.50#	0.12 ± 0.07#

*$P < 0.05$ *vs* CTRL
#$P < 0.05$ *vs* STZ
UPE = Urinary Protein Excretion
ACR = Albumin Creatinine *Ratio*
CrCl = Creatinine Clereance

3.3 JNJ39758979 prevents glomerular structure alterations

The beneficial effects displayed by JNJ39758979 on renal function were accompanied and supported by the maintenance of tissue morphological structure. As reported in Fig. 2, the mesangial matrix expansion induced by STZ ($n = 10$/group, $P < 0.05$) was significantly reduced in a dose-dependent manner by JNJ39758979. Interestingly, the presence of nodule lesions found in the STZ-treated animals was consistent with the development of nodular sclerosis described in the III class classification of glomerular lesions in diabetic nephropathy [30]. The lesion was still identified in the animals treated with JNJ39758979 at 25 mg/kg, but not in the 50 mg/kg or in the 100 mg/kg groups (Fig. 2). These results confirmed the efficacy of JNJ39758979 at inhibiting diabetic nephropathy development.

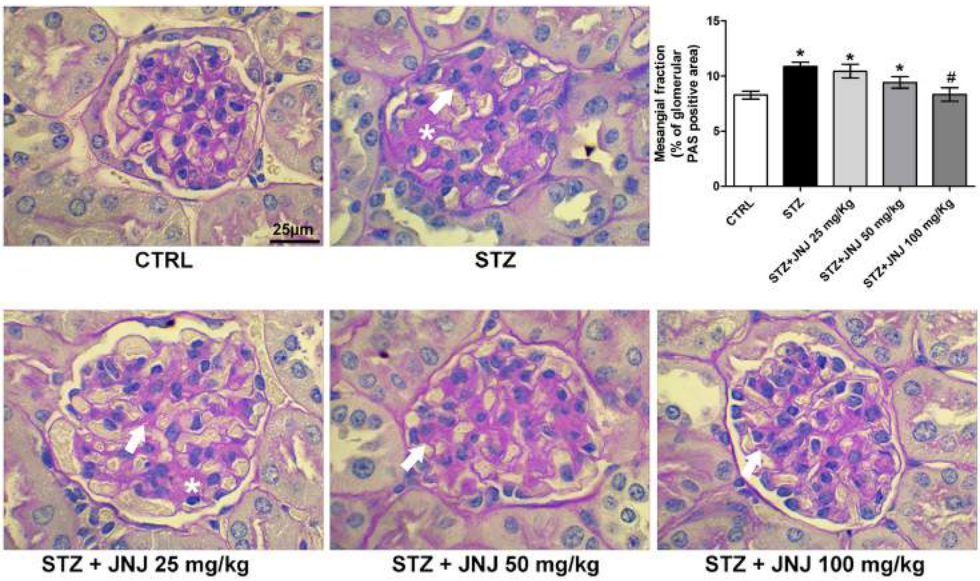

Fig. 2. Effect evoked by JNJ39758979 on morphological lesions. PAS staining from renal sections. Arrows highlight mesangial matrix expansion while stars indicate nodular lesions. Micrographs at 100X magnification are representative of 10 animals/group. The densitometric analysis is expressed as the mean ± S.E.M. ($n = 10$); *$P < 0.05$ *vs* CTRL, °$P < 0.05$ *vs* STZ.

The electron microscopy analysis reported in Fig. 3 showed pathological glomerular alterations in STZ mice coherent with the disease model used. In particular, the quantitative analysis performed on the glomerular filtration barrier clearly confirmed a significant increase in podocyte foot process loss, as showed by the increased foot process base width (Fig. 3b; $P < 0.05$) with a parallel reduction in the number of foot processes (Fig. 3c; $P < 0.05$) and slit diaphragm (SD)/10 µm (Fig. 3d; $P < 0.05$). JNJ39758979 prevented the glomerular structure alterations induced by STZ in a dose-dependent manner, with the highest doses effective on podocyte effacement (Fig. 3; $P < 0.05$).

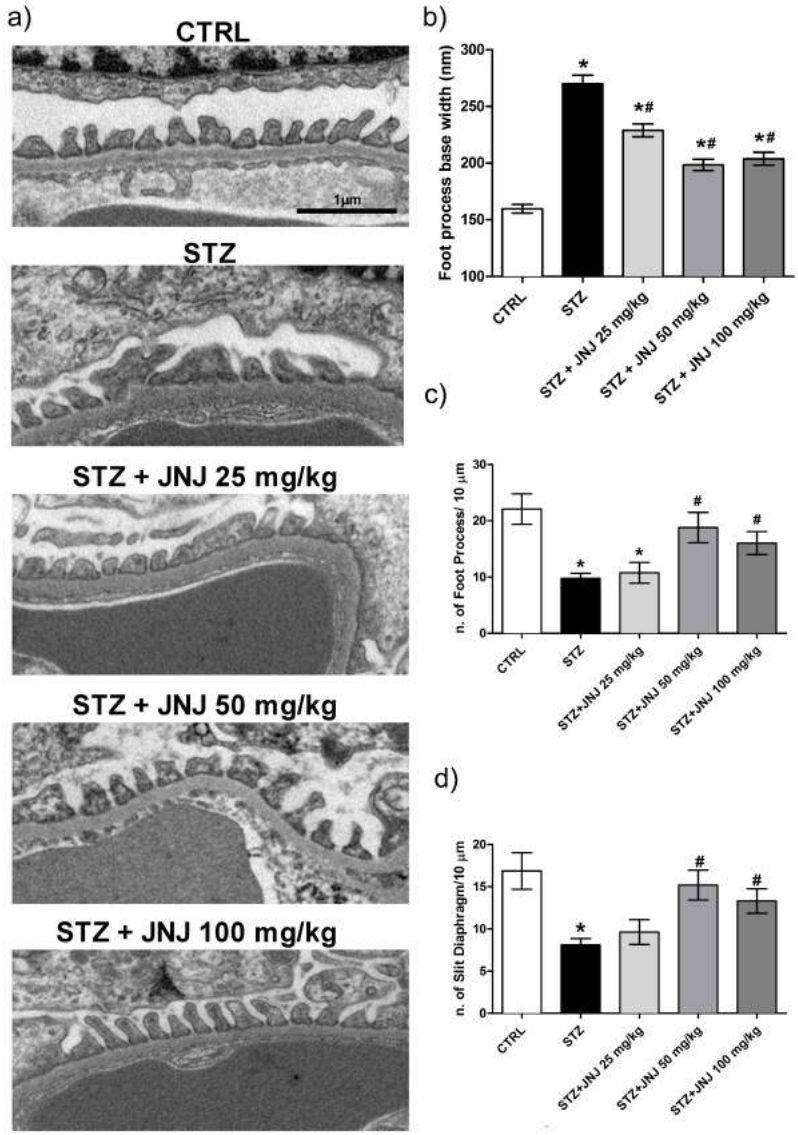

Fig. 3. Effect evoked by JNJ39758979 on glomerular morphology. EM micrographs showing ultrathin podocyte sections. Micrographs at 20K magnification are representative of 10 animals/group (**a**). Foot processes base width (**b**), number of podocyte foot processes/10 μm of GMB (**c**) and (**d**) number of SD/10 μm were quantified. The densitometric analysis is expressed as the mean ± S.E.M. ($n = 10$); *$P < 0.05$ *vs* CTRL, #$P < 0.05$ *vs* STZ.

3.4 JNJ39758979 prevents renal fibrosis decreasing inflammation process

The pathological alterations we observed have been correlated with an affected glomerular hemodynamic caused by a pro-inflammatory milieu. Based on the well-known role of histamine in inflammation and the contribution of H_4R in polymorphonuclear neutrophils (PMNs) chemotaxis [31], we evaluated the effect of JNJ39758979 on the renal presence of infiltrating immune cells. H&E staining, shown in Fig. 4a, revealed a profound increase in renal cellularity, consisting with infiltration, in STZ mice. The administration of JNJ39758979 reduced the hyper-cellularity, irrespective of the dosage. Consistent with inflammatory cell infiltration, STZ mice showed a pronounced interstitial fibrosis demonstrated by collagen fibre deposition (Fig. 4b). The treatment with JNJ39758979 at 50 and 100 mg/kg significantly blunted the collagen deposition induced by STZ ($n = 10$/group, $P < 0.05$).

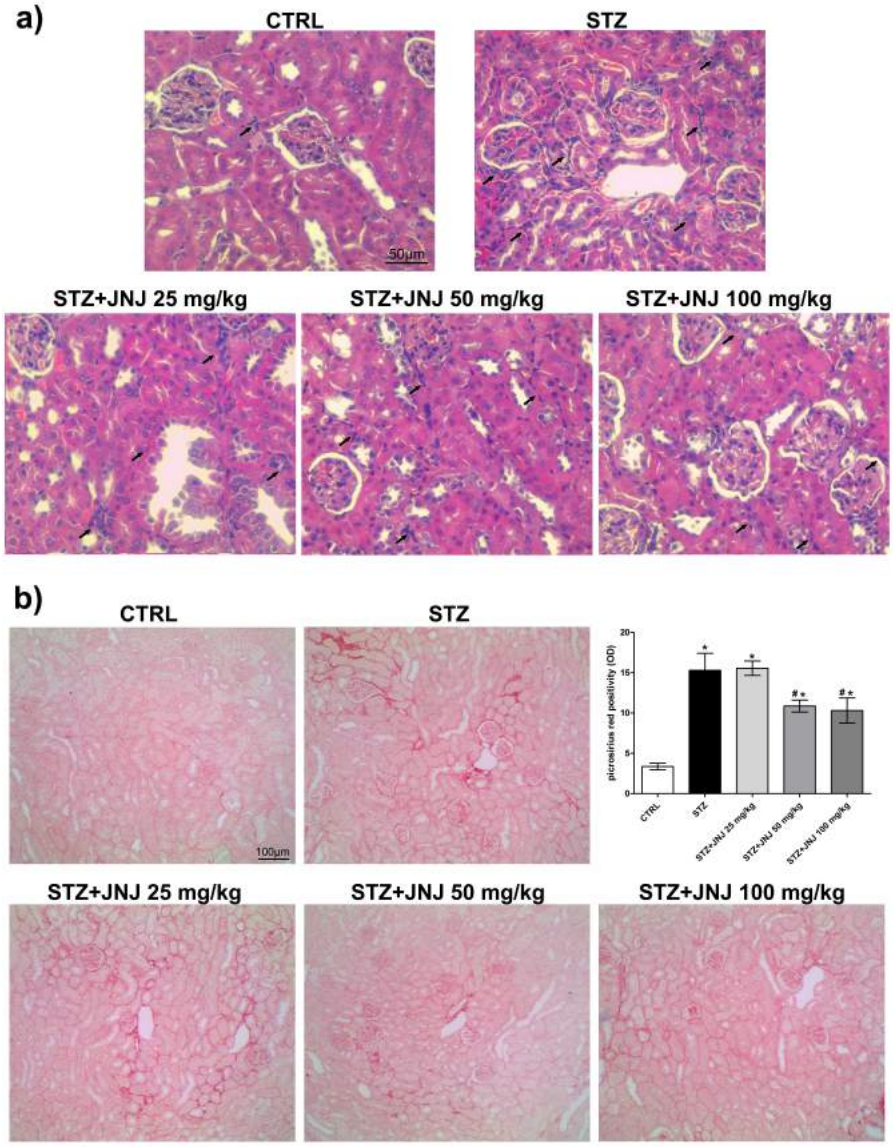

Fig. 4. Effect evoked by JNJ39758979 on tubular interstitial infiltration and renal fibrosis. (**a**) Hematoxylin/Eosin staining from renal sections. Arrows highlight infiltrating cells. Micrographs at 25X magnification are representative of 10 animals/group. (**b**) Collagen deposition in the renal interstitium evaluated by picrosirius red stating. Micrographs at 10X magnification are

representative of 10 animals/group. The densitometric analysis is expressed as the mean ± S.E.M. ($n = 10$); *$P < 0.05$ *vs* CTRL, °$P < 0.05$ *vs* STZ.

3.5 Effect of JNJ39758979 on tubular reabsorption processes

The immunofluorescence analysis of histamine H_4R demonstrated a clear tubular localization of this receptor, which was expressed on the proximal tubules as demonstrated by its co-presence with the proximal tubule marker, AQP1 (Fig 5). Interestingly, no co-localization was found with THP, marker of the thick ascending limb of the loop of Henlé, or AQP2, marker of the principal cells of the collecting duct (Fig 5).

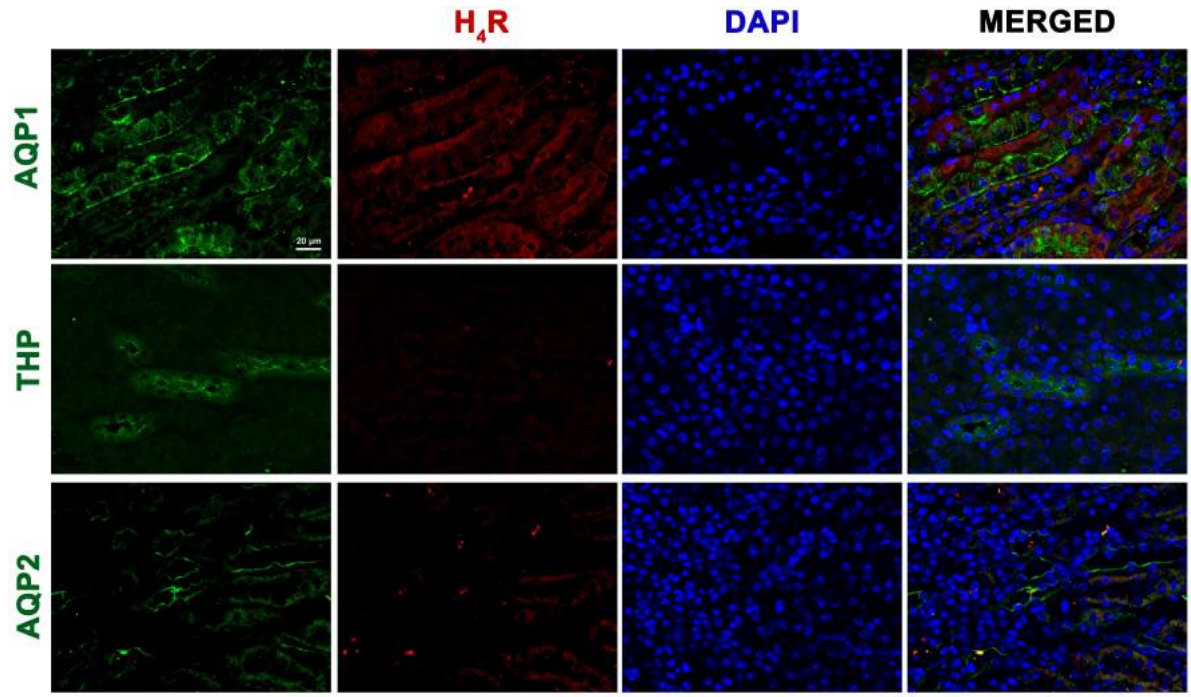

Fig. 5. H_4R tubular expression in DBA2/J mice. Immunofluorescence stain showing co-localization of H_4R (red) with AQP1-, THP- or AQP2-positive cells (green). Nuclei were stained with DAPI (blue). Micrographs at 40X magnification are representative of 10 animals.

Therefore, a possible direct effect of JNJ39758979 on tubular reabsorptive process was investigated. As shown in Fig. 6, JNJ39758979 was able to prevent the reduction in megalin mRNA (Fig. 6a) and protein expression (Fig. 6b and 6c) induced by STZ, irrespective of the dosage (n = 10/group, $P < 0.05$), thus suggesting a direct effect of the drug tested on tubular reabsorption. As megalin expression is inversely correlated with that of NHE3 [32], we also evaluated the effect of JNJ39758979 on the expression of this important exchanger. Consistently, the drug at 50 and 100 mg/kg was effective in preventing the up-regulation of NHE3 expression induced by STZ (n = 5/group, $P < 0.05$; Fig. 6d).

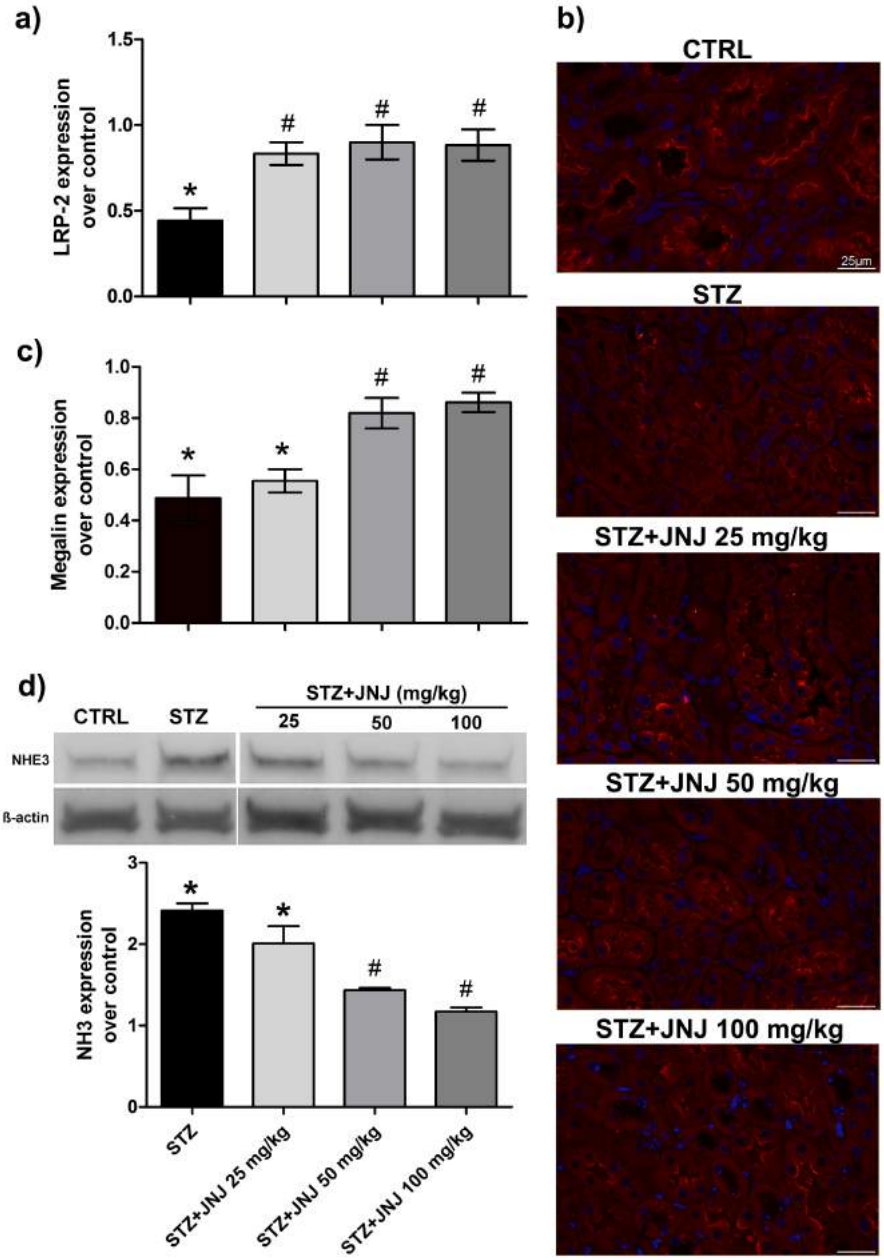

Fig. 6. Effect evoked by JNJ39758979 on megalin tubular expression. LRP-2 expression by qPCR was determined on kidney specimens. Results are expressed as mean ± S.E.M. of in 10 animals/group; *$P < 0.05$ *vs* CTRL, °$P < 0.05$ *vs* STZ (**a**). Megalin expression on tubular epithelial cells was determined by immunofluorescence analysis. Micrographs at 40X magnification are representative of 10 animals/group (**b**). Densitometric analysis of Megalin expression determined by immunofluorescence analysis. Expression levels over control are expressed as the mean ± S.E.M. ($n = 10$); *$P < 0.05$ *vs* CTRL, °$P < 0.05$ *vs* STZ (**c**). NHE3 expression in kidney tissue was determined by immunoblotting; representative radiograph is shown. Expression levels, normalized to β-actin, are expressed as fold-increase over control, mean ± S.E.M. of 5 animals/group; *$P < 0.05$ *vs* CTRL, °$P < 0.05$ *vs* STZ (**d**).

4 Discussion and Conclusions

The data herein reported demonstrate a potential beneficial effect of H_4R antagonism on the progression of diabetic nephropathy. This study was based on the assumption that the renal content of histamine, due to an increase in HDC activity, as well as H_4R expression [6], are boosted in a diabetic condition [12, 13]. These two conditions also occurred in our present mouse model (Supplementary Fig. 1 and Fig. 2a). Interestingly, we confirmed the epithelial renal cells as a local source of histamine. Indeed, as reported in Supplementary Fig. 1 and consistent with previous data in the literature [9-11], HDC enzyme is expressed by residential cells both within the glomerulus and the tubules.

In this present study the H_4R antagonism was achieved by the JNJ39758979, a compound whose preclinical profile has already been characterised and the dose-response effects observed in this study were similar to that seen in other chronic models[33, 34]. The drug was administered using a preventive protocol, starting at the early onset of diabetes. Therefore, our study implicates a key role for H_4R in diabetic nephropathy progression. Moreover, our data reveal a direct contribution of H_4R antagonism in preserving renal integrity and function. Indeed, JNJ39758979 did not affect either the glycaemic status or the catabolic status of diabetic mice, but it was effective in counteracting the alterations of renal function parameters, such as ACR and CrCl.

The dose-dependent reduction in both ACR and CrCl parameters provides strong evidence for a direct involvement of the H_4R in regulating tubular reabsorption mechanism(s), consistent with the tubular distribution of the H_4R, previously demonstrated by our group [6, 8] and, herein, further confirmed. Interestingly, in DBA2/J mice the H_4R co-localized with AQP1, marker of the proximal tubule epithelial cells. A similar localization was reported for humans [8], but not for rats [6]. Therefore, the already observed widespread inter-species differences in H_4R expression [6, 8] has been once confirmed once again.

The hypothesis of a direct involvement of the H_4R in regulating tubular reabsorption mechanism(s) is further strengthened by the ability of JNJ39758979 to preserve megalin expression down-regulated by STZ. The maintenance of megalin expression on the apical domain of tubular epithelial cells has been suggested as an important defence mechanism. Indeed, megalin preserves and reclaims albumin throughout tubular reabsorption [35]. An increase in tubular reabsorption has been recognised as a defence mechanism following hyperfiltration [36]. Therefore, according to the "tubule-centric" hypothesis of diabetic nephropathy etiopathogenesis [37], megalin sustained expression could represent one of the mechanisms by which JNJ39758979 is able to maintain the structural integrity of the glomerulus. The effect on NHE3, a Na^+/H^+ exchanger on renal proximal tubules, could account for the prevention of both urinary acidosis and albuminuria observed for JNJ39758979 at 100 mg/kg. Interestingly, our data furnish the first evidence for a role of JNJ39758979 in regulating H^+ efflux/transport across membranes. JNJ39758979 reduced NHE3 expression in diabetic mice. Interestingly, this transporter is under the strict regulation of the renin-angiotensin-system (RAS) and the inhibition of the RAS system has been previously demonstrated to affect NHE3 expression; in particular, losartan was reported to reduce NHE3 expression in opossum kidney (OKP) cells [38]. Looking at the pathways involved in both the AT_1 and H_4R signalling, interesting similarities could be noted, e.g. both being G_i-coupled protein receptors.

Therefore, analogous to the AT_1/G_i pathway [38], we could speculate that the NHE3 expression at the proximal tubular level could be modulated by the H_4R/G_i pathway [39, 40]. Moreover, independent, although contrasting, evidence is suggestive of interplay between RAS and histamine. For instance, histamine has been reported to stimulate renin release from the isolated perfused rat kidney [17], but H_4R was reported to inhibit cardiac mast cell renin release in ischemia/reperfusion [41]. Therefore, it is possible that the effect of JNJ39758979 on NHE3 expression could be secondary to RAS modulation.

Interestingly, these studies allow further speculations about the multifarious roles of histamine in acid/base homeostasis. Indeed, the properties of this amine in the gastric acid balance through H_2R are well recognised since H_2R antagonists entered the market as anti-acid drugs many years ago. More recently, it was also demonstrated that H_3R activation in cardiac sympathetic nerves results in decreased NHE3 activity [42].

Collectively, the ability of JNJ39758979 to affect megalin and NHE3 expression is suggestive of a preserved ability to concentrate urine. The drug at 100 mg/kg was able to significantly decrease water to urine *ratio*, which was profoundly different in normal and diabetic animals, with the first excreting around 25% and the latter around 80% of their water intake. These data strongly supports the mechanistic hypothesis based on the beneficial effect of the compound tested on renal re-uptake. JNJ39758979 displayed a dose-dependent effect in reducing the urine volume, although the basal level was not restored. Notably, as no statistical differences were observed in the glycaemic level between the different diabetic groups, a direct effect on the proximal tubule, more than the diabetes status, could account for the urine volume reduction observed. Indeed, the tubule fluid that is delivered to the distal nephron mostly determines the volume of dilute urine that can be excreted. The tubular reabsorption enhancement results in a reduction of the fluids delivered to the distal tubule, which itself limits the rate of water excretion [43]. Therefore, we can assume that H_4R activation, preserving the proximal tubule reabsortive machinery caused a reduction in urine volume, without any anti-hyperglycaemic effect. The balance between H_4R and H_3R activity in the kidney could explain the partial efficacy of H_4R antagonism in restoring the basal urine volume. Interestingly, we demonstrated that renal H_3R is predominantly localized on the collecting duct epithelium [7], a major regulator of water reabsorption. Moreover, its expression was up-regulated in the kidney of both diabetic rats [7] and DBA2/J mice (Supplementary Fig. 2b), and in a pilot study H_3R expression in mice positively correlated with urine volume [22]. Therefore, it is possible to speculate subsequent to blockade of the H_4R, the free histamine binds to the H_3R in the collecting duct, thus explaining the partial efficacy of H_4R antagonism in restoring the basal urine volume.

A persistent inflammatory environment due to robust inflammatory cells recruitment is recognised as one of the major causes of collagen deposition and fibrosis development. Indeed, GFR decline is associated with the presence in urine and serum of specific inflammatory markers, such as interleukin (IL)-6, monocyte chemoattractant protein (MCP)1, and interferon gamma-induced protein (IP)-10 [44]. Interestingly, both glomeruli and tubules play active roles in process. Within the glomerulus, podocytes can be considered immune-like cells as they constitutively express Toll-like receptor 4, which can induce the costimulatory molecule B7.1 expression [45]. Furthermore,

podocytes can stimulate specific $CD4^+$ and $CD8^+$ T cell responses, mimicking some of the functions of dendritic cells or macrophages of hematopoietic origin [46], thus promoting an inflammatory and fibrotic state. On the other side, tubulointerstitial injury contributes to the development of diabetic nephropathy. In our study, the establishment of tubular interstitial fibrosis sustains the functional injury induced by STZ. Inhibiting the induction of pro-inflammatory and pro-fibrotic mediators have already been demonstrated to have renoprotective effects [47]. H_4R blockade has been reported to exert anti-fibrotic effects through the reduction in transforming growth factor (TGF)-ß production and pro-inflammatory events in a model of lung fibrosis [48, 49]. Besides TGF-ß, ATP is a known pro-fibrotic stimulus that may regulate renal fibroblast proliferation and activity, thus influencing fibroblast to myofibroblast transformation [50], and it is also involved in the inflammatory process via histamine release [51]. Moreover, the inhibition of chemotaxis by H_4R antagonism is well documented for several immune cell types. Accordingly, we found a reduced cellular infiltration in the tubular interstitium following JNJ39758979 administration, whose higher doses were effective in reducing the excess of extracellular matrix collagen deposition.

In conclusion, our data suggest that the H_4R participates in diabetic nephropathy through both a direct effect on tubular reabsorption, which could lead to an effect on glomerular integrity, and an indirect action on renal tissue architecture through inflammatory cell recruitment. Therefore H_4R antagonism emerges as a possible therapeutic approach to counteract diabetic nephropathy development.

Acknowledgments

This work was funded by the Ateneo/CSP2012 (H4 Histamine Receptor As A New Pharmacological Target For The Treatment Of Diabetic Nephropathy – HISDIAN), University of Turin (ex60% 2014) and University of Florence (ex60% 2015).

A preliminary report of this study was presented at the *45th Annual Meeting of the European Histamine Research Society (EHRS), Florence, Italy, May 11–14, 2016* and *at the 52nd EASD Annual Meeting, Munich, Germany, September 12-16, 2016*, whose abstract have been published on *Inflammation Research 2016 July; 65 (Suppl 1) and Diabetologia 2016 August; 59 (Suppl 1), respectively*. We acknowledge Dr. Janet Chazot for her editorial assistance on the manuscript.

Authorship contributions is listed as follow: AP, PLC, ACR conceived and designed the study; CG and RS animal care and housing; EV, CG, MA, RC and DG acquired and analysed the data; AP, ACR interpreted the data; AP, GC, ACR drafted the article and revised it critically for important intellectual content; RLT provided the final approval of the version to be published.

Conflict of interest

RLT is employed by the Jansen Research and Development, LLC. No other conflict of interests exist.

References

[1] L. Guariguata, D.R. Whiting, I. Hambleton, J. Beagley, U. Linnenkamp, J.E. Shaw, Global estimates of diabetes prevalence for 2013 and projections for 2035, Diabetes research and clinical practice 103(2) (2014) 137-49.
[2] J. Chen, Diabetic Nephropathy: Scope of the Problem, in: L. E.V., B. V. (Eds.), Diabetes and Kidney Disease, Springer Science+Business Media New York2014, pp. 9-14.
[3] H. Suzuki, T. Kikuta, T. Inoue, U. Hamada, Time to re-evaluate effects of renin-angiotensin system inhibitors on renal and cardiovascular outcomes in diabetic nephropathy, World journal of nephrology 4(1) (2015) 118-26.
[4] A.J. Collins, R.N. Foley, B. Chavers, D. Gilbertson, C. Herzog, K. Johansen, B. Kasiske, N. Kutner, J. Liu, W. St Peter, H. Guo, S. Gustafson, B. Heubner, K. Lamb, S. Li, S. Li, Y. Peng, Y. Qiu, T. Roberts, M. Skeans, J. Snyder, C. Solid, B. Thompson, C. Wang, E. Weinhandl, D. Zaun, C. Arko, S.C. Chen, F. Daniels, J. Ebben, E. Frazier, C. Hanzlik, R. Johnson, D. Sheets, X. Wang, B. Forrest, E. Constantini, S. Everson, P. Eggers, L. Agodoa, 'United States Renal Data System 2011 Annual Data Report: Atlas of chronic kidney disease & end-stage renal disease in the United States, American journal of kidney diseases : the official journal of the National Kidney Foundation 59(1 Suppl 1) (2012) A7, e1-420.
[5] A. Pini, I. Obara, E. Battell, P.L. Chazot, A.C. Rosa, Histamine in diabetes: Is it time to reconsider?, Pharmacological research 111 (2016) 316-24.
[6] A.C. Rosa, C. Grange, A. Pini, M.A. Katebe, E. Benetti, M. Collino, G. Miglio, D. Bani, G. Camussi, P.L. Chazot, R. Fantozzi, Overexpression of histamine H(4) receptors in the kidney of diabetic rat, Inflammation research : official journal of the European Histamine Research Society ... [et al.] 62(4) (2013) 357-65.
[7] A. Pini, P.L. Chazot, E. Veglia, A. Moggio, A.C. Rosa, H_3 receptor renal expression in normal and diabetic rats, Inflammation research : official journal of the European Histamine Research Society ... [et al.] 64(5) (2015) 271-273.
[8] E. Veglia, C. Grange, A. Pini, A. Moggio, C. Lanzi, G. Camussi, P.L. Chazot, A.C. Rosa, Histamine receptor expression in human renal tubules: a comparative pharmacological evaluation, Inflammation research : official journal of the European Histamine Research Society ... [et al.] 64(3-4) (2015) 261-270.
[9] E. Veglia, A. Pini, A. Moggio, C. Grange, F. Premoselli, G. Miglio, K. Tiligada, R. Fantozzi, P.L. Chazot, A.C. Rosa, Histamine type 1-receptor activation by low dose of histamine undermines human glomerular slit diaphragm integrity, Pharmacological research 114 (2016) 27-38.
[10] M.A. Beaven, S. Jacobsen, Z. Horakova, Modification of the enzymatic isotopic assay of histamine and its application to measurement of histamine in tissues, serum and urine, Clin Chim Acta 37 (1972) 91-103.
[11] T.K. Morgan, K. Montgomery, V. Mason, R.B. West, L. Wang, M. van de Rijn, J.P. Higgins, Upregulation of histidine decarboxylase expression in superficial cortical nephrons during pregnancy in mice and women, Kidney Int 70(2) (2006) 306-14.
[12] R.A. Markle, T.M. Hollis, A.J. Cosgarea, Renal histamine increases in the streptozotocin-diabetic rat, Exp Mol Pathol 44(1) (1986) 21-8.

[13] D.S. Gill, C.S. Thompson, P. Dandona, Histamine synthesis and catabolism in various tissues in diabetic rats, Metabolism 39(8) (1990) 815-8.
[14] R.J. Sinclair, R.D. Bell, M.J. Keyl, Effects of prostaglandin E2 (PGE2) and histamine on renal fluid dynamics, Am J Physiol 227(5) (1974) 1062-6.
[15] R.O. Banks, J.D. Fondacaro, M.M. Schwaiger, E.D. Jacobson, Renal histamine $H_1$and H_2receptors: characterization and functional significance, Am J Physiol 235(6) (1978) F570-5.
[16] I. Ichikawa, B.M. Brenner, Mechanisms of action of hisamine and histamine antagonists on the glomerular microcirculation in the rat, Circ Res 45(6) (1979) 737-45.
[17] U. Schwertschlag, E. Hackenthal, Histamine stimulates renin release from the isolated perfused rat kidney, Naunyn Schmiedebergs Arch Pharmacol 319(3) (1982) 239-42.
[18] S.G. Gurgen, D. Erdogan, G. Take-Kaplanoglu, The effect of histamine on kidney by fasting in rats, Bratislavske lekarske listy 114(5) (2013) 251-7.
[19] B.M. Ruger, Q. Hasan, N.S. Greenhill, P.F. Davis, P.R. Dunbar, T.J. Neale, Mast cells and type VIII collagen in human diabetic nephropathy, Diabetologia 39(10) (1996) 1215-22.
[20] J.M. Zheng, G.H. Yao, Z. Cheng, R. Wang, Z.H. Liu, Pathogenic role of mast cells in the development of diabetic nephropathy: a study of patients at different stages of the disease, Diabetologia 55(3) (2012) 801-11.
[21] Reena, T. Kaur, A. Kaur, M. Singh, H.S. Buttar, D. Pathak, A.P. Singh, Mast cell stabilizers obviate high fat diet-induced renal dysfunction in rats, European journal of pharmacology 777 (2016) 96-103.
[22] A. Pini, P.L. Chazot, A.C. Rosa, Parallel hierarchical intra-strain difference between the susceptibility to diabetic nephropahty and renal histamine receptor expression, Inflammation research : official journal of the European Histamine Research Society ... [et al.] 65(Suppl 1) (2016) s45.
[23] B.M. Savall, F. Chavez, K. Tays, P.J. Dunford, J.M. Cowden, M.D. Hack, R.L. Wolin, R.L. Thurmond, J.P. Edwards, Discovery and SAR of 6-alkyl-2,4-diaminopyrimidines as histamine H(4) receptor antagonists, Journal of medicinal chemistry 57(6) (2014) 2429-39.
[24] R.L. Thurmond, B. Chen, P.J. Dunford, A.J. Greenspan, L. Karlsson, D. La, P. Ward, X.L. Xu, Clinical and preclinical characterization of the histamine H(4) receptor antagonist JNJ-39758979, The Journal of pharmacology and experimental therapeutics 349(2) (2014) 176-84.
[25] Kelsey J.L., Whittemore A.S., Evans A.S., T. D, Methods in Observational Epidemiology, Second ed., Oxford University Press, Oxford, 1996.
[26] L.S. Ramagli, Quantifying protein in 2-D PAGE solubilization buffers, Methods in molecular biology 112 (1999) 99-103.
[27] S.R. Dunn, Z. Qi, E.P. Bottinger, M.D. Breyer, K. Sharma, Utility of endogenous creatinine clearance as a measure of renal function in mice, Kidney Int 65(5) (2004) 1959-67.
[28] P.S. Yuen, S.R. Dunn, T. Miyaji, H. Yasuda, K. Sharma, R.A. Star, A simplified method for HPLC determination of creatinine in mouse serum, American journal of physiology. Renal physiology 286(6) (2004) F1116-9.

[29] K.K. Wu, Y. Huan, Streptozotocin-induced diabetic models in mice and rats, Current protocols in pharmacology Chapter 5 (2008) Unit 5 47.
[30] T.W. Tervaert, A.L. Mooyaart, K. Amann, A.H. Cohen, H.T. Cook, C.B. Drachenberg, F. Ferrario, A.B. Fogo, M. Haas, E. de Heer, K. Joh, L.H. Noel, J. Radhakrishnan, S.V. Seshan, I.M. Bajema, J.A. Bruijn, S. Renal Pathology, Pathologic classification of diabetic nephropathy, Journal of the American Society of Nephrology : JASN 21(4) (2010) 556-63.
[31] S. Mommert, S. Kleiner, M. Gehring, B. Eiz-Vesper, H. Stark, R. Gutzmer, T. Werfel, U. Raap, Human basophil chemotaxis and activation are regulated via the histamine H4 receptor, Allergy 71(9) (2016) 1264-73.
[32] A.C. Girardi, F. Di Sole, Deciphering the mechanisms of the Na+/H+ exchanger-3 regulation in organ dysfunction, American journal of physiology. Cell physiology 302(11) (2012) C1569-87.
[33] R.L. Thurmond, P.J. Desai, P.J. Dunford, W.P. Fung-Leung, C.L. Hofstra, W. Jiang, S. Nguyen, J.P. Riley, S. Sun, K.N. Williams, J.P. Edwards, L. Karlsson, A potent and selective histamine H4 receptor antagonist with anti-inflammatory properties, The Journal of pharmacology and experimental therapeutics 309(1) (2004) 404-13.
[34] R. Kiss, G.M. Keseru, Novel histamine H4 receptor ligands and their potential therapeutic applications: an update, Expert opinion on therapeutic patents 24(11) (2014) 1185-97.
[35] L.E. Dickson, M.C. Wagner, R.M. Sandoval, B.A. Molitoris, The proximal tubule and albuminuria: really!, Journal of the American Society of Nephrology : JASN 25(3) (2014) 443-53.
[36] A. Saito, T. Takeda, H. Hama, Y. Oyama, K. Hosaka, A. Tanuma, R. Kaseda, M. Ueno, S. Nishi, S. Ogasawara, F. Gondaira, Y. Suzuki, F. Gejyo, Role of megalin, a proximal tubular endocytic receptor, in the pathogenesis of diabetic and metabolic syndrome-related nephropathies: protein metabolic overload hypothesis, Nephrology 10 Suppl (2005) S26-31.
[37] M.E. Williams, Diabetic nephropathy: the proteinuria hypothesis, American journal of nephrology 25(2) (2005) 77-94.
[38] G.D. Queiroz-Leite, M.C. Peruzzetto, E.A. Neri, N.A. Reboucas, Transcriptional regulation of the Na(+)/H(+) exchanger NHE3 by chronic exposure to angiotensin II in renal epithelial cells, Biochemical and biophysical research communications 409(3) (2011) 470-6.
[39] K.L. Morse, J. Behan, T.M. Laz, R.E. West, Jr., S.A. Greenfeder, J.C. Anthes, S. Umland, Y. Wan, R.W. Hipkin, W. Gonsiorek, N. Shin, E.L. Gustafson, X. Qiao, S. Wang, J.A. Hedrick, J. Greene, M. Bayne, F.J. Monsma, Jr., Cloning and characterization of a novel human histamine receptor, The Journal of pharmacology and experimental therapeutics 296(3) (2001) 1058-66.
[40] I.J. de Esch, R.L. Thurmond, A. Jongejan, R. Leurs, The histamine H4 receptor as a new therapeutic target for inflammation, Trends in pharmacological sciences 26(9) (2005) 462-9.
[41] S. Aldi, K. Takano, K. Tomita, K. Koda, N.Y. Chan, A. Marino, M. Salazar-Rodriguez, R.L. Thurmond, R. Levi, Histamine H4-receptors inhibit mast cell renin release in ischemia/reperfusion via protein kinase C epsilon-dependent aldehyde dehydrogenase type-2 activation, The Journal of pharmacology and experimental therapeutics 349(3) (2014) 508-17.
[42] R.B. Silver, C.J. Mackins, N.C. Smith, I.L. Koritchneva, K. Lefkowitz, T.W. Lovenberg, R. Levi, Coupling of histamine H3 receptors to neuronal Na+/H+ exchange: a novel protective

mechanism in myocardial ischemia, Proceedings of the National Academy of Sciences of the United States of America 98(5) (2001) 2855-9.
[43] J.G. Verbalis, T. Berl, Disorders of water balance, in: B.M. Brenner (Ed.), Brenner & Rector's The kidney, Saunders, Philadelphia, 2008, pp. 459-504.
[44] A.S. Krolewski, Progressive renal decline: the new paradigm of diabetic nephropathy in type 1 diabetes, Diabetes care 38(6) (2015) 954-62.
[45] R. Bassi, A. Fornoni, A. Doria, P. Fiorina, CTLA4-Ig in B7-1-positive diabetic and non-diabetic kidney disease, Diabetologia 59(1) (2016) 21-9.
[46] A. Goldwich, M. Burkard, M. Olke, C. Daniel, K. Amann, C. Hugo, C. Kurts, A. Steinkasserer, A. Gessner, Podocytes are nonhematopoietic professional antigen-presenting cells, Journal of the American Society of Nephrology : JASN 24(6) (2013) 906-16.
[47] M.W. Taal, B.M. Brenner, Renoprotective benefits of RAS inhibition: from ACEI to angiotensin II antagonists, Kidney Int 57(5) (2000) 1803-17.
[48] A.C. Rosa, A. Pini, L. Lucarini, C. Lanzi, E. Veglia, R.L. Thurmond, H. Stark, E. Masini, Prevention of bleomycin-induced lung inflammation and fibrosis in mice by naproxen and JNJ7777120 treatment, The Journal of pharmacology and experimental therapeutics 351(2) (2014) 308-16.
[49] L. Lucarini, A. Pini, A.C. Rosa, C. Lanzi, M. Durante, P.L. Chazot, S. Krief, A. Schreeb, H. Stark, E. Masini, Role of histamine H4 receptor ligands in bleomycin-induced pulmonary fibrosis, Pharmacological research 111 (2016) 740-8.
[50] A. Solini, V. Usuelli, P. Fiorina, The dark side of extracellular ATP in kidney diseases, Journal of the American Society of Nephrology : JASN 26(5) (2015) 1007-16.
[51] E.S. Schulman, M.C. Glaum, T. Post, Y. Wang, D.G. Raible, J. Mohanty, J.H. Butterfield, A. Pelleg, ATP modulates anti-IgE-induced release of histamine from human lung mast cells, American journal of respiratory cell and molecular biology 20(3) (1999) 530-7.

Supplementary Materials

Creatinine evaluations

Twenty-five µl of plasma or 5 µl of urine were exposed to cold acidified acetonitrile (1:200 v/v glacial acetic acid: acetonitrile) in a *ratio* of 1:4. After precipitation and dehydration of the sample, creatinine was re-suspended in 25 µl of HPLC mobile phase (2.00 l of 5 mM sodium acetate and adjusted to pH 4.2 ± 0.1 with 1.4 ml glacial acetic acid; following filtration, 80 ml of methanol and 20 ml of acetonitrile were added). All reagents were HPLC grade or better. HPLC was performed by a L2 Binary Pump, instrument with a UV-vis spectrophotometer detector (LC 95 PerkinElmer; Akron, OH, USA). A polar bonded-phase column Zorbax 300-SCX column (2.1 x 50 mm, 5 µm; Agilent Technology, Santa Clara, CA, USA). The flow was set at 0.3 ml min^{-1}, runtime was 10 minutes. Detection of eluting creatinine peak was achieved at 225 nm at 3.65 ± 0.02 minutes. The concentration of creatinine was determined from an external standard regression line (8 points, from 0.003 to 1.000 mg/dl). The analysis was performed in duplicate.

Morphological analysis quantification

PAS positive area, indicating matrix mesangial expansion, were analysed using the ImageJ 1.33 image analysis program (http://rsb.info.nih.gov/ij) upon selection of an appropriate threshold. Values are reported as PAS positive glomerulus area compared to the total glomerular area; measurements of at least 40 glomeruli for each animal from the different experimental groups were performed.

Optical density measurements of the deep red–stained collagen fibres were carried out by using the ImageJ 1.33 image analysis program (http://rsb.info.nih.gov/ij) upon selection of an appropriate threshold to include the specific stained tissue and guarantee the exclusion of non-collagen areas. Values, reported as arbitrary units, are calculated as surface area × optical density × 10^{-6}; the measurements of at least 20 images for individual animals were performed.

Megalin immunofluorescence quantification

The optical density of ROI was evaluated with the ImageJ 1.33 image analysis program (http://rsb.info.nih.gov/ij) upon selection of an appropriate threshold to include the positive area. As described above, values, reported as megalin expression over control, are calculated as surface area × optical density × 10^{-6}; the measurements of at least 50 images for individual animals were performed.

RNA isolation

Total RNA was isolated by chloroform/phenol RNA extraction with TRIzol Reagent according with the manufacturer's instructions. DNA contamination was removed with DNase (Deoxiribonuclease I) prior to the reverse transcription (RT) reaction. The concentration and purity of total RNA were evaluated prior and after the DNase treatment by spectrophotometry, measuring the absorbance at 260 and 280 nm wavelength. The absence of RNA degradation was confirmed by agarose gel electrophoresis with ethidium bromide staining.

Immunoistochemistry for HDC detection

Conventional immunohistochemical procedures were employed for the HDC enzyme were employed. Briefly, immunoperoxidase staining was performed on 5 μm section for formalin-fixed tissue using an appropriate antigen retrieval (10 mM sodium citrate, pH 6.0). After incubation in 1.5% bovine serum albumin in PBS, pH 7.4 for 20 min at RT to minimise non-specific binding, renal sections were incubated overnight at 4 °C with rabbit polyclonal anti-HDC (1:50; HPA038891 Sigma Aldrich). The immunoreactions were revealed by incubation with the secondary biotinylated anti-rabbit (Vector Laboratories, Inc.; Burlingame, CA, USA) antibodyfollowed by a three-layer streptavidin–biotin–peroxidase complex staining method (Vectastain ABC Elite kit and 3',3-diaminobenzadine tetrahydrochloride, DAB; Vector Laboratories, Inc.). Negative controls were carried out by omitting the primary antiserum. Stomach corpus from mice was used as positive control. All sections were stained or immunostained in a single session to minimize artifactual differences in the staining. Stained sections were examined, and pictures were taken with an Zeiss Axioskop microscope (Zeiss, Mannheim, DE) at 10X or 25X magnification, respectively.

Immunofluorescence for H_1R and H_2R detection

After antigen retrieval and blocking, 5 µm kidney paraffin sections were incubated overnight with goat polyclonal anti-H_1R (sc-33967, lot number L0913; Santa Cruz Biotechnology) or with rabbit polyclonal anti-H_2R (349–358, produced and validated in the School of Biological and Biomedical Sciences, Durham University; 1 µg/ml), followed by incubation with the Alexa Fluor 594 AffiniPure bovine anti-goat or the Alexa Fluor 594 AffiniPure donkey anti-rabbit (1:350) for 2 h. After counterstaining with DAPI, photomicrographs were obtained by a confocal laser-scanning microscope The immunoreaction products were observed under an epifluorescence Zeiss Axioskop microscope at 40X magnification.

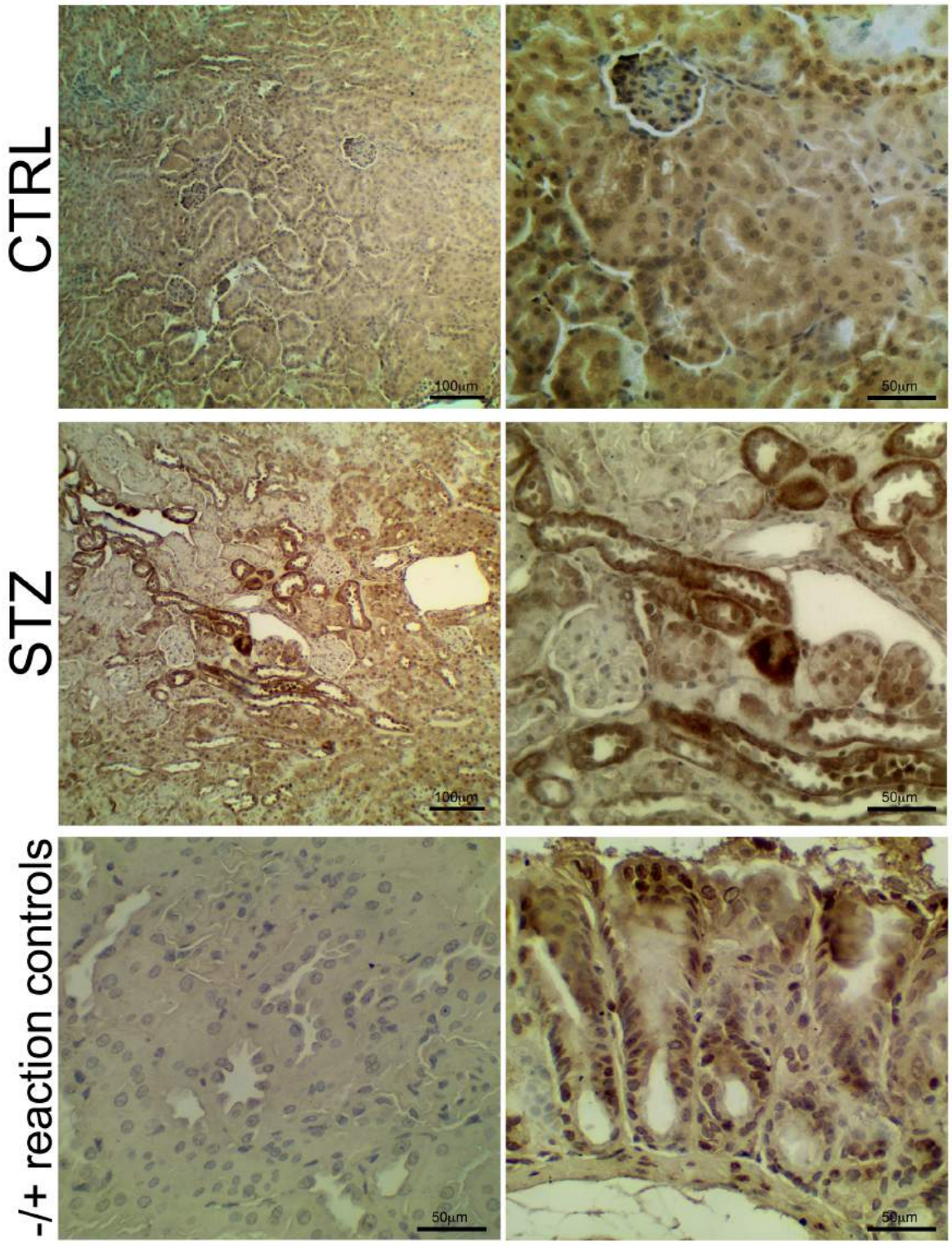

Supplementary Fig. 1 HDC expression. Kidney sections from control or STZ-treated mice immunolabelled with specific anti-HDC antibody. Negative controls were carried out on kidney sections by omitting the primary antiserum. Stomach corpus from mice was used as positive control. Micrographs at 10X magnification are representative of 10 animals/group.

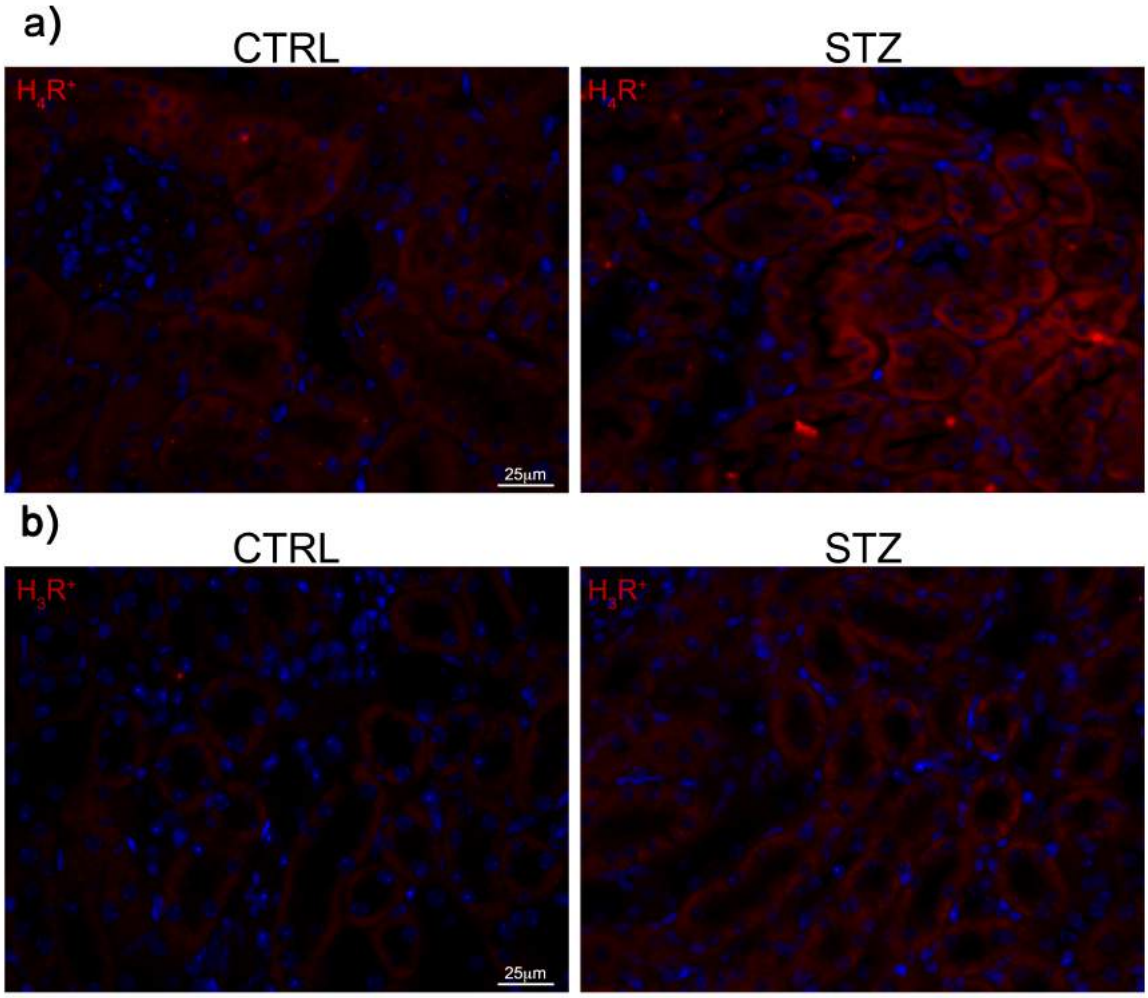

Supplementary Fig. 2 H_4R and H_3R renal expression. Kidney sections from control or STZ-treated mice immunolabelled with specific anti-H_4R (a) or H_3R (b) antibodies. Nuclei were stained with DAPI (blue). Micrographs at 40X magnification are representative of 10 animals/group.